Biochimica et Biophysica Acta 1840 (2014) 2091–2104

Contents lists available at ScienceDirect

Biochimica et Biophysica Acta

journal homepage: www.elsevier.com/locate/bbagen

Generating novel recombinant prokaryotic lectins with altered carbohydrate binding properties through mutagenesis of the PA-IL protein from *Pseudomonas aeruginosa*

Damien Keogh [a,1], Roisin Thompson [a,b,1], Ruth Larragy [a,b], Kenneth McMahon [a], Michael O'Connell [a], Brendan O'Connor [a,b], Paul Clarke [a,b,*]

[a] School of Biotechnology, Dublin City University, Glasnevin, Dublin 9, Ireland
[b] Irish Separation Science Cluster (ISSC), National Centre for Sensor Research (NCSR), Dublin City University, Glasnevin, Dublin 9, Ireland

ARTICLE INFO

Article history:
Received 29 July 2013
Received in revised form 17 December 2013
Accepted 13 January 2014
Available online 22 January 2014

Keywords:
LecA
N-acetyl-lactosamine
Galectins
Lectinology
Glycoprotein analysis
Glycoprotein purification

ABSTRACT

Background: Prokaryotic lectins offer significant advantages over eukaryotic lectins for the development of enhanced glycoselective tools. Amenability to recombinant expression in *Escherichia coli* simplifies their production and presents opportunities for further genetic manipulation to create novel recombinant prokaryotic lectins (RPLs) with altered or enhanced carbohydrate binding properties. This study explored the potential of the α-galactophilic PA-IL lectin from *Pseudomonas aeruginosa* for use as a scaffold structure for the generation of novel RPLs.
Method: Specific amino acid residues in the carbohydrate binding site of a recombinant PA-IL protein were randomly substituted by site-directed mutagenesis. The resulting expression clones were then functionally screened to identify clones expressing rPA-IL proteins with altered carbohydrate binding properties.
Results: This study generated RPLs exhibiting diverse carbohydrate binding activities including specificity and high affinity for β-linked galactose and N-acetyl-lactosamine (LacNAc) displayed by N-linked glycans on glycoprotein targets. Key amino acid substitutions were identified and linked with specific carbohydrate binding activities. Ultimately, the utility of these novel RPLs for glycoprotein analysis and for selective fractionation and isolation of glycoproteins and their glycoforms was demonstrated.
Conclusions: The carbohydrate binding properties of the PA-IL protein can be significantly altered using site-directed mutagenesis strategies to generate novel RPLs with diverse carbohydrate binding properties.
General significance: The novel RPLs reported would find a broad range of applications in glycobiology, diagnostics and in the analysis of biotherapeutics. The ability to readily produce these RPLs in gram quantities could enable them to find larger scale applications for glycoprotein or biotherapeutic purification.

1. Introduction

Lectins are proteins that are capable of recognizing and binding reversibly to specific oligosaccharide (glycan) structures displayed on cell surfaces and glycoproteins [1–3]. Since their initial discovery, lectins have found diverse applications [4], but with the growing interest in the field of glycobiology lectins have come to the forefront as important analytical and diagnostic tools helping to elucidate the basis of complex biological processes and disease states [5,6]. Lectins display exquisite specificity for cognate ligands, and their ability to bind to glycans *in situ* facilitates interrogation of the glycosylation status of a sample without the prior need for glycan release and derivatization [1]. Labelled lectins are widely used in glycoanalytical procedures such as lectin blotting and ELLAs that are analogous to the standard ELISA [7–10]. Lectin arrays, which represent powerful tools enabling high throughput glycoanalysis, are increasingly being reported in the literature for a diverse range of applications including cancer diagnostics [6,11–16]. Through immobilization onto solid support media, the ability of lectins to discriminate between different glycan structures can be harnessed to effect the separation and selective purification of glycoproteins and their glycoforms. Lectin affinity chromatography (LAC) is now commonly used in laboratories for glycoprotein purification and is often used as an initial step to pre-concentrate glycopeptides, or separate glycoforms, prior to MS-based glycoanalysis [17–19].

The most commonly used lectins are plant derived, but these have a number of significant limitations. These eukaryotic lectins can be structurally complex and often require post-translational modifications, including glycosylation, or disulfide bond formation [1,2]. As a result of

Abbreviations: PA-IL, *Pseudomonas aeruginosa* lectin 1; PA-ILU, untagged native PA-IL; rPA-IL, recombinant PA-IL; 6HIS, affinity purification tag comprised of 6 tandem histidine residues; ELLA, enzyme linked lectin assay; iGb3, isoglobotriaosylceramide (Galα1–3Galβ1–4Glc); PBS, Phosphate Buffered Saline; TBS, Tris Buffered Saline; TBST, Tris Buffered Saline with Tween 20; IPTG, Isopropyl-β-D-thiogalactopyranoside

* Corresponding author at: School of Biotechnology, Dublin City University (DCU), Glasnevin, Dublin 9, Ireland. Tel.: +353 1 700 5961; fax: +353 1 7005412.
E-mail address: Paul.Clarke3@gmail.com (P. Clarke).
[1] Authors made equal contribution to the work reported.

0304-4165/$ – see front matter © 2014 Elsevier B.V. All rights reserved.
http://dx.doi.org/10.1016/j.bbagen.2014.01.020

this, eukaryotic lectins are often not amenable to recombinant production, particularly in *Escherichia coli* based systems which are the systems of choice for such purposes [20]. While many attempts have been made to produce plant lectins recombinantly, these frequently result in the production of insoluble proteins and very low yields [20,21]. Consequently, plant lectins are usually purified from source materials by conventional liquid chromatography techniques, and it is from here that many of their limitations stem. The quality, specificity and activity of these lectins can vary from one supplier to another and from batch to batch depending on the quality of the starting material and the purification methods used in their preparation [6,20]. These inconsistencies in performance complicate applications for glycoprotein analysis, particularly in relation to their use for diagnostic purposes. In addition, the need to purify from source material means that only limited quantities of these lectins can be obtained, and the final lectin preparations can be expensive [20]. These issues have restricted the use of lectins to analytical scale applications where large quantities are not generally required.

While lectins are ubiquitous in nature, prokaryotic lectins present unique opportunities for the development of new glycoselective bioaffinity tools. Most of these advantages stem from their greater amenability to production in *E. coli* as recombinant prokaryotic lectins (RPLs). In addition to facilitating simplified production, recombinant approaches enable the modification and optimization of lectin binding specificities and affinities [22–24] as well as opportunities to facilitate orientation specific immobilization to generate enhanced glycoanalytical platforms [25]. Despite their many advantages, prokaryotic lectins have to date remained largely underexploited, but there is now growing interest in the exploitation of these new lectin sources as they have the potential to redress the many shortcomings of the traditional plant lectins and lead to more sensitive and robust glycoanalytical and diagnostic tools [20].

The PA-IL protein is one of two soluble lectins produced by the opportunistic pathogen *Pseudomonas aeruginosa* (Fig. 1) [26,27]. The binding specificity of this lectin has been examined extensively using a broad spectrum of methodologies, and it has been shown to bind preferentially to glycans with terminal α-linked galactose and not to bind significantly to glycans with terminal β-linked galactose [28]. The PA-IL protein is known to exhibit relative resistance to heating, extreme pH and proteolysis [27] and therefore embodies ideal physiochemical properties as a template scaffold protein structure for the generation of novel robust glycoanalytical tools. This study explored the potential of the PA-IL protein for the generation of novel RPLs with altered or enhanced carbohydrate binding properties. It demonstrated that the carbohydrate binding specificity of the PA-IL protein could be significantly altered by introducing random substitutions at specific amino acid residues in the protein's carbohydrate binding site. Novel RPLs displaying diverse carbohydrate binding properties, including specificity and high affinity for glycans with terminal β-linked galactose and N-acetyl-lactosamine (LacNAc) displayed by N-linked glycans on glycoprotein targets, were successfully generated. Some of these RPLs displayed affinities for these glycan epitopes significantly greater than that of the equivalent commercially available plant lectin ECL (*Erythrina cristagalli* Lectin) [21,29]. The functional characterization of a collection of these RPLs enabled the identification of specific amino acid substitutions linked with observed carbohydrate binding properties. Ultimately, the utility of these novel RPLs for simple and highly sensitive glycoprotein analysis, without the need for prior labelling, was demonstrated. Through immobilization onto sepharose resins and magnetic particles, we demonstrated the utility of these RPLs for efficient glycoselective fractionation and isolation of glycoproteins and their glycoforms. The ability to produce these RPLs in large quantities and to very high levels of purity via cost-effective and scalable protocols could enable them to overcome the limitations of plant and other eukaryotic lectins and to potentially find large-scale applications for the selective purification of glycoproteins and glycosylated biotherapeutics.

2. Materials and methods

2.1. Plasmid construction—pQE30PA-IL & pQE60PA-IL

All strains and plasmids used or constructed as part of this study are listed and described in Table 1. The *lecA* gene encoding the PA-IL protein was amplified from *P. aeruginosa* PAO1 genomic DNA by PCR to facilitate cloning into the pQE series of *E. coli* expression vectors from Qiagen. PCR reactions were carried out using high fidelity Phusion Taq and PCR conditions recommended by the manufacturer (New England BioLabs). The *lecA* gene was amplified using primers PA-IL-F1 [5′- AAAAGGATCCATGG CTTGGAAAGGTGAGG-3′] and PA-IL-R1 [5′-AAAAAAGCTTTCACGACT GATCCTTTCCAATATT-3′] which generated a product that could be cloned as a BamHI-HindIII fragment into the pQE30 expression vector. The resulting plasmid, pQE30PA-IL (Supplementary Fig. 1A), expressed a recombinant PA-IL protein (rPA-IL) with an amino terminal 6HIS tag (rPA-ILN). The *lecA* gene was also amplified using primers PA-IL-F2

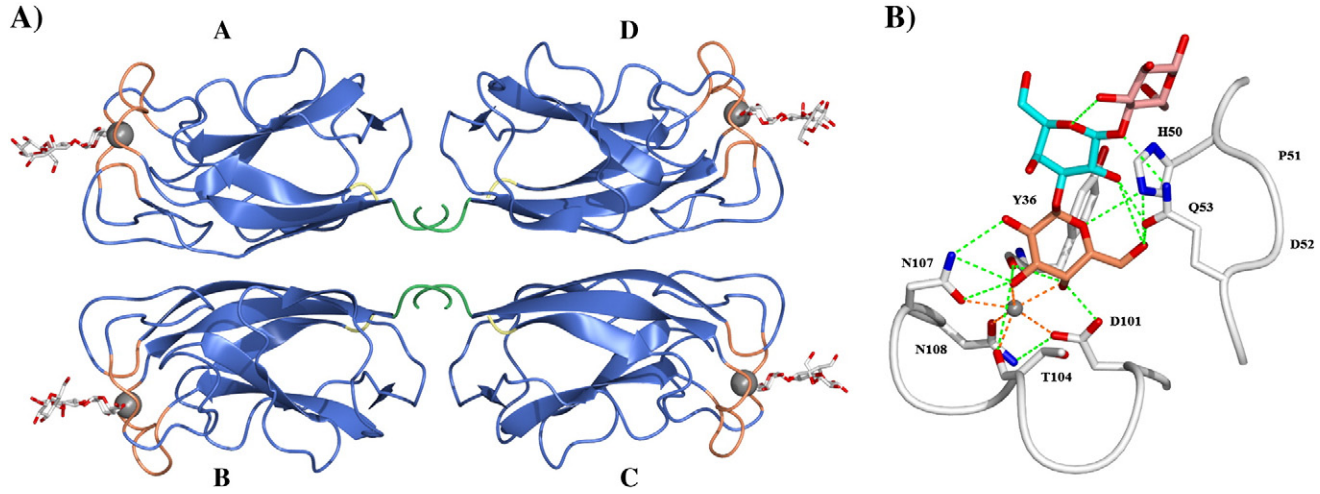

Fig. 1. Structure of the PA-IL protein and its carbohydrate binding site. (A) Tetrameric PA-IL protein with bound iGb3 trisaccharide Galα1–3Galβ1–3Glc (PDB code 2VXJ) [28]. Each monomer subunit contains a single carbohydrate binding site. A single calcium ion is coordinated within each binding site (grey sphere) and is essential for sugar binding. Residues involved in calcium coordination and carbohydrate binding are highlighted (Orange). The C-terminus and N-terminus of each monomer are highlighted (Green and Yellow respectively). (B) The PA-IL binding site showing coordination of the calcium ion and binding of iGb3. Amino acid residues involved in calcium coordination (Red lines) and contributing to the formation of hydrogen bonds (Green lines) with bound iGb3 are indicated. Images were generated using Deep View (Swiss Model) [50] and rendered using CCP4MG software [51].

Table 1
Strains and plasmids used in this study.

Strains	Genotype	Description	Source
Escherichia coli			
JM109	F′traD36, *pro*AB + *lacI*^{q}, Δ*lacZ* M15, *end*A1, *rec*A1, *hsd*R17(r_k-, m_k+), *mcr*A, *sup*E44, λ- *gyr*A96, *rel*A1 Δ*(lacproAB), thi-1.*	All purpose cloning strain, produces stable plasmid DNA.	Promega
KRX	[F′, *tra*D36, Δ*omp*P, *pro*A + B+, *lacI*^{q}, Δ(*lacZ*)M15] Δ*omp*T, *end*A1, *rec*A1, *gyr*A96 (Nalr), *thi-1*, *hsd*R17 (r_k–, m_k+), *rel*A1, *sup*E44, Δ(*lac-pro*AB), Δ(*rha*BAD)::T7 RNA polymerase.	Protease-deficient protein expression host.	Promega [30]
Pseudomonas aeruginosa			
PAO1	Wild-type genomic DNA		Dr. M. O'Connell
Plasmids	Features	Description	Source
pQE30	T5 promoter/*lac* operator element, *rrnB* T1 transcriptional termination region, ColE1 origin, β-lactamase gene.	Expresses proteins with an N-terminal RGS-6HIS affinity tag.	Qiagen
pQE60	T5 promoter/*lac* operator element, *rrnB* T1 transcriptional termination region, ColE1 origin, β-lactamase gene.	Expresses proteins with a C-terminal 6HIS affinity tag.	Qiagen
pQE30PA-IL	pQE30 with cloned *P. aeruginosa lecA*	Expresses rPA-ILN: Wild-type PA-IL with an N-terminal RGS-6HIS affinity tag.	This work
pQE60PA-IL	pQE60 with cloned *P. aeruginosa lecA*	Expresses rPA-ILC: Wild-type PA-IL with a C-terminal 6HIS affinity tag.	This work
Mutagenized plasmids	Amino acid substitutions	Protein expressed	Source
pPC30PA-IL-A8	H50L D52H Q53R	rPA-ILNmA8	This work
pPC30PA-IL-B4	H50T D52N Q53R	rPA-ILNmB4	This work
pPC30PA-IL-B10	H50V D52C Q53E	rPA-ILNmB10	This work
pPC30PA-IL-C5	H50N D52T Q53S	rPA-ILNmC5	This work
pPC30PA-IL-E6	H50N D52N Q53G	rPA-ILNmE6	This work
pPC30PA-IL-E12	H50G D52C Q53R	rPA-ILNmE12	This work
pPC30PA-IL-F3	H50V D52C Q53R	rPA-ILNmF3	This work
pPC30PA-IL-F6	H50P D52R Q53L	rPA-ILNmF6	This work
pPC30PA-IL-G3	H50V D52N Q53N	rPA-ILNmG3	This work

[5′-AAAACCATGGCTTGGAAAGGTGAGGTT CTGG-3′] and PA-IL-R2 [5′-AAAAAGATCTCGACTGATCCTTTCCAATATTGACAC-3′] to enable cloning as an NcoI-BglII fragment into the pQE60 vector (Qiagen). The resulting plasmid, pQE60PA-IL (Supplementary Fig. 1B), expressed an rPA-IL protein with a carboxy terminal 6HIS tag (rPA-ILC).

2.2. Protein expression and purification

For protein expression, plasmids were transformed into the protease-deficient *E. coli* strain KRX [30]. Expression clones were cultured at 30 °C in Terrific Broth (TB) and protein expression induced by addition of IPTG to a final concentration of 50 μM. Cells were harvested by centrifugation and cell pellets resuspended in lysis buffer (50 mM NaH_2PO_4, 300 mM NaCl, 40 mM imidazole, pH 8.0). Cell disruption was achieved by high pressure using a Constant Systems cell disrupter, and cell debris was removed by centrifugation. Clarified cell lysates were applied to 10 mL IMAC columns (IMAC Hypercel from Pall Life Sciences), and a high stringency wash buffer with 80 mM imidazole was used to remove non-specifically bound contaminating proteins. The desired 6HIS tagged rPA-IL proteins were ultimately eluted using 500 mM imidazole, and eluted proteins were aliquoted and stored at −80 °C in the elution buffer. Purified proteins were analysed by SDS-PAGE to assess purity (Fig. 2) and routinely buffer exchanged and concentrated using Vivaspin centrifugal membrane devices (Sartorius-Stedim), with a molecular weight cutoff of 10 kDa, according to manufacturer's guidelines. Protein concentration was estimated by measuring absorbance at 280 nm, and typical yields were approximately 200 mg per 250 mL starting culture.

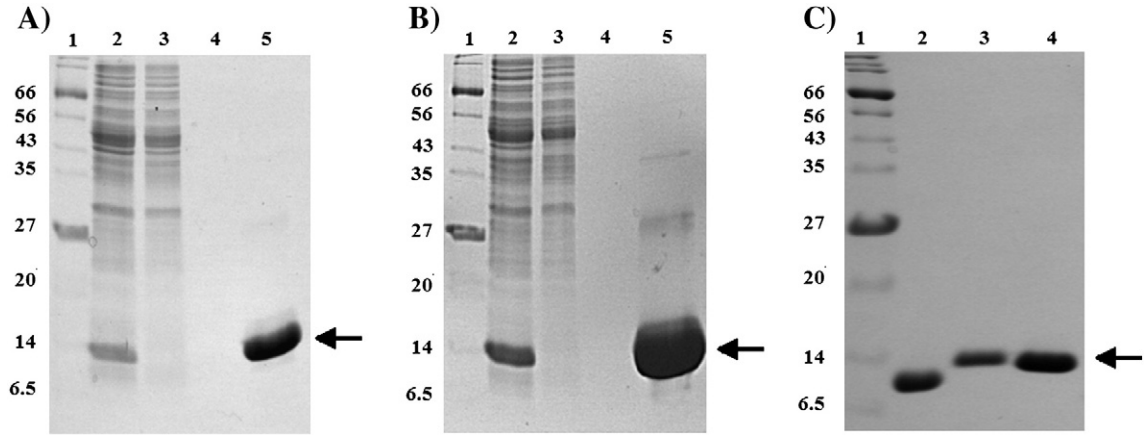

Fig. 2. SDS-PAGE analysis of PA-IL proteins: Panels (A) and (B) show SDS-PAGE analysis of samples from the expression and purification of rPA-ILC and rPA-ILN respectively. In each panel: Lane 1—molecular weight ladder (NEB Wide Range Protein Ladder—sizes are in kDa); Lane 2—soluble cell lysate (CL); Lane 3—final sample of flow through cell lysate (FT); Lane 4—final sample of 80 mM imidazole wash; Lane 5—eluted rPA-IL protein. The rPA-IL proteins (←) ran at approximately 14 kDa as expected. (C) Comparison of purified rPA-IL proteins with commercial untagged PA-IL (PA-ILU). Lane 1—SDS-PAGE protein standards; Lane 2—PA-ILU; Lane 3—rPA-ILN; Lane 4—rPA-ILC.

2.3. Gel permeation chromatography (GPC)

The estimated molecular weights of the rPA-IL proteins were determined by GPC which was performed on a Superdex 75 10/300 GL column (GE Healthcare) using an AKTA Purifier 100 FPLC system. The molecular weight of commercially obtained untagged PA-IL (PA-ILU), purchased from Sigma Aldrich, was also experimentally determined and used for comparison with 6HIS tagged rPA-IL proteins to enable determination of their quaternary structure (Supplementary Fig. 2).

2.4. Hemagglutination assays

This assay is widely used to study lectin activity and is dependent on the multi-valency typically displayed by lectins. The assay was essentially performed according to the method described by Garber et al. [31]. The assay was performed using papain-treated rat red blood cells (RBCs), obtained from the Bioresource unit at DCU, such that the final concentration of cells in reaction wells was 3.5% w/v. Lectins to be tested were prepared in TBS (20 mM Tris, 150 mM NaCl, 1 mM $CaCl_2$, 1 mM $MnCl_2$, 1 mM $MgCl_2$, pH 7.6). Hemagglutination was observed, after 1 h incubation at 25 °C, as a thin film of cells coating the bottom of wells in U-bottomed 96 well plates compared to a concentrated spot of sedimented cells observed in negative controls to which no lectin was added (Supplementary Fig. 3A). One hemagglutination unit (HU) was defined as the minimum quantity of lectin required to fully agglutinate the RBC solution. Sugar inhibition assays were performed such that the final lectin concentration in reaction wells was equivalent to 2 HU (Supplementary Fig. 3B).

2.5. Site-directed mutagenesis of the rPA-ILN protein

PCR-based site-directed mutagenesis of the *lecA* gene was achieved through whole vector amplification (inverse PCR) in which the pQE30PA-IL vector was used as the parental template DNA. Whole vector amplification was achieved using the primers PA-ILmutF [5′-CGTTTT GTGGTGCGCTGGTCATGAAG ATTGGC-3′] and PA-ILmutR [5′-CGTCGT GGCAGATCAGCCCNNNNNNCGGNNNCTCCCGATCG CCCTG-3′]. These primers were 5′ phosphorylated and designed to anneal within the *lecA* sequence with their 5′ ends exactly next to each other. The reverse primers were designed to overlap the region to be mutagenized enabling the introduction of mutations through manipulation of reverse primer sequences (Supplementary Fig. 1C). Successful PCR reactions were purified and subjected to digestion with the restriction enzyme DpnI. This restriction enzyme only cleaves its restriction site (GATC) when there is N6-methylation of the adenine residue. Plasmid DNA isolated from dam^+ *E. coli* strains carry such methylation, and so this restriction enzyme selectively digested parental template DNA while leaving newly amplified PCR products, lacking methylation, intact. Digestions were ultimately run on agarose gels to ensure separation of any digested parental vector DNA fragments from the newly synthesized and mutagenized PCR products. PCR products corresponding to the expected size of linear vector were gel extracted. The final purified PCR products, with blunt phosphorylated ends, were re-circularized by simple self ligation and the ligated DNA transformed into *E. coli* strain KRX.

2.6. Assembly and screening of matrices of clones expressing mutagenized rPA-ILN proteins

Transformants carrying mutagenized pPC30PA-IL vectors were picked into sterile deep well (2 mL) 96 well plates to generate master plates of mutant clones expressing mutagenized rPA-ILN proteins (rPA-ILNm). Each plate carried 77 independent mutant clones. The remaining wells in each plate were used for internal controls. These included KRX expressing parental rPA-ILN, KRX expressing no lectin and empty media wells to monitor for any contamination during subculturing of plates. The remaining wells left empty in each plate enabled inclusion of commercial plant lectins as controls in subsequent ELLA screens. Master plates were used to inoculate fresh 96 well plates containing 600 μL of LB media supplemented with ampicillin (100 μg/mL) and IPTG (50 μM) to induce expression of rPA-ILNm proteins. After overnight incubation at 30 °C, cells were harvested by centrifugation and subsequently disrupted chemically by resuspending cell pellets in 1X Cell Lytic B solution (Sigma–Aldrich) by repeated gentle pipetting. Plates were then incubated at room temperature for 1 h or overnight at 4 °C to allow disruption of cells. Cell debris was removed by centrifugation, and cell lysates were diluted 10 fold using TBST prior to being screened by ELLA.

2.7. General enzyme linked lectin assay (ELLA) method

The neoglycoproteins used were from Dextra Laboratories: Galα1–2Gal–BSA, Galα1–3Gal–BSA, Galβ1–3GalNAc–HSA (HSA–T-antigen), Galβ1–4GlcNAc–BSA (BSA–LacNAc), GalNAc–BSA, GlcNAc–BSA, Fuc–BSA, Man–BSA. These neoglycoproteins present on average 10 to 12 carbohydrate moieties per protein molecule. Oligosaccharide moieties are linked via a 3 carbon atom spacer while monosaccharides are linked by a 14 carbon atom spacer. The link between the carbohydrate and the protein is in the β-anomeric configuration. Glycoproteins used were from Sigma–Aldrich. The glycoprotein glycoforms asialotransferrin, agalactotransferrin and agalactofetuin were generated by treatment of parental glycoproteins with neuraminidase (*Clostridium perfingens*) and β1–4 galactosidase (*Bacteroides fragilis*) in accordance with manufacturer's guidelines (New England Biolabs). Biotinylated plant lectins ECL (*E. cristagalli* Lectin), GSLI (*Griffonia simplicifolia* isolectin B4) and SNA (*Sambucus nigra* Agglutinin) were from Vector Laboratories. The inhibitory sugars N-acetyl-lactosamine (LacNAc) and lactose-N-biose were from Elicityl, and all other sugars were from Sigma–Aldrich.

ELLAs were essentially performed according to the method described by Thompson et al. (2011) [8]. Briefly, glycoproteins and neoglycoproteins were prepared in PBS and immobilized in assay plates by addition of 50 μL of solution to each well followed by overnight incubation at 4 °C. Lectin binding was performed by addition of 50 μL of lectin test solutions to wells followed by one hour incubation at 25 °C. For qualitative ELLAs, lectin solutions were prepared at a concentration of 2 μg/mL in TBST (20 mM Tris, 150 mM NaCl, 0.05% Tween-20, 1 mM $CaCl_2$, 1 mM $MnCl_2$, 1 mM $MgCl_2$, pH 7.6). For lectin dose–response curves, each lectin was evaluated at a range of concentrations, and test solutions were prepared by serial 1:1 dilution of an initial lectin solution of 10 μg/mL to a final concentration of 156 ng/mL. For inhibition studies serially diluted inhibitory carbohydrates were mixed with an equal volume of lectin to generate reaction mixtures in which the final lectin concentration was 0.2 μg/mL. After 30 min incubation at 25 °C, 50 μL of lectin–inhibitor mixtures was subjected to binding assays against a specific neoglycoprotein target as usual. Lectin binding was detected using 50 μL of HRP conjugated antibody (Sigma–Aldrich) diluted 1:10,000 in TBST and incubation for 1 h at 25 °C. The 6HIS tagged rPA-IL proteins were detected using an anti-HIS antibody, while biotinylated plant lectins were detected using an anti-biotin antibody. Bound antibody was detected using a tetramethylbenzidine (TMB) substrate prepared by dissolving TMB tablets according to manufacturer's guidelines. This solution was diluted 1:1 prior to use, and subsequently 90 μL of this final solution was added to wells of ELLA plates. Reactions were allowed to proceed for 5 min before being stopped using 50 μL of a 10% H_2SO_4 solution. All assays were performed in triplicate. Data points shown in figures therefore represent average values obtained, and the standard deviation (SD) typically did not exceed 5%. For semi-quantitative assays (lectin dose–response curves), data was analysed using BIAevaluation software (version 4.0.1) and a 4 parameter equation to generate fitted curves.

2.8. Activity assessment of rPA-IL protein preparations

The percentage activity of purified rPA-ILNm protein preparations used in characterization studies was assessed by affinity chromatography using an asialofetuin sepharose column. Asialofetuin was prepared in coupling buffer (20 mM Na_2HPO_4, 500 mM NaCl, pH 8.5) and mixed with NHS-Sepharose (GE Healthcare) at a concentration of approximately 10 mg/mL of resin. This mixture was then left mixing by inversion overnight at 4 °C. Unbound protein was decanted, and unreacted groups on the resin were capped with 1 M ethanolamine in coupling buffer at pH 8.5. This was left mixing by inversion at room temperature for 4 h. Finally, the resin was subjected to four successive washes with coupling buffer and acetate buffer (100 mM NaOAc, 500 mM NaCl, pH 4.0) to remove non-specifically bound protein. Asialofetuin was observed to immobilize with high efficiency, and the resulting resin was estimated to have approximately 10 mg of asialofetuin per mL of resin. The resin was packed into a 1 mL FPLC cartridge (FliQ Column Housings, Generon) to enable easy connection to an ÄKTA Purifier 100 FPLC system and equilibrated using TBS prior to use. To assess rPA-ILNm lectin preparations, a sample of each lectin was injected onto the column to fractionate inactive (unbound) and active (bound) protein. Runs were performed at a flow rate of 0.2 mL per minute, and bound rPA-ILNm proteins were eluted using 0.5 M galactose prepared in TBS (Supplementary Fig. 4). Percentage activity was determined through quantification of unbound and bound protein fractions.

2.9. Lectin affinity constant determination by ELLA

Affinity constants were essentially determined according to the method described by Kirkeby et al. 2002 [10]. ELLAs were performed as outlined previously using a constant concentration of 2 μg/mL for the rPA-ILNm proteins and 4 μg/mL of ECL to ensure all lectins were evaluated at equimolar concentrations. Each lectin was evaluated against a dilution series of a Galβ1–4GlcNAc–BSA (BSA–LacNAc) neoglycoprotein with a concentration range from 10 μg/mL to 19.5 ng/mL (prepared by serial 1:1 dilution of a 10 μg/mL stock). Immobilization was achieved by aliquoting 50 μL of each dilution in the series into the wells of assay plates. All assays were performed in triplicate. Plotted data represents average values obtained, and the standard deviation was typically less than 5%. Data was analysed using BIAevaluation software and curve fitting performed using a 4 parameter equation. The resulting neoglycoprotein dose–response curve obtained enabled the calculation of B_{max} and the affinity constant K_D for each lectin for the neoglycoprotein. B_{max} is defined as being the maximum plateau value of absorption and represents the maximum number of lectin binding sites expressed in the units of the Y-axis (AU). K_D is defined as being the neoglycoprotein concentration required to fill half of the available lectin binding sites at equilibrium and was therefore the neoglycoprotein concentration that generated a signal equivalent to half B_{max}. The unit for K_D is neoglycoprotein concentration expressed in μg/mL or molarity (nM). These values are specific for the defined experimental conditions used.

2.10. Fabrication and evaluation of RPL affinity sepharose columns and magnetic particles

RPL affinity resins were prepared by immobilization onto cyanogen bromide (CNBr) activated Sepharose 4B following the same procedure as outlined for the preparation of asialofetuin resin with the exception that RPL was mixed with resin at a concentration of 30 mg per mL of resin. RPL immobilization densities of approximately 20 mg/mL of resin were typically achieved. RPL affinity resins were packed into 1 mL FPLC cartridges and equilibrated using TBS. Glycoprotein samples were prepared in TBS, and 2 mL sample volumes were injected onto the 1 mL RPL affinity columns and typically run at a flow rate of 0.5 mL per minute. Bound glycoproteins were eluted using 0.5 M galactose prepared in TBS. For small-scale isolation of glycoproteins, RPLs were immobilized at a density of 10 mg/mL onto NHS-derivatized magnetic particles according to the manufacturer's instructions (Merck-Millipore PureProteome™ magnetic particles). To perform pull down assays, 50 μL of RPL-beads was mixed with 100 μL of a test protein mixture and mixed by inversion for 1 h. Unbound protein was then removed, and the particles were washed with four 1 mL aliquots of TBST. Bound protein was eluted by addition of 100 μL of TBST with 0.5 M galactose followed by incubation for 1 h.

3. Results

3.1. Production of affinity tagged recombinant PA-IL (rPA-IL)

Commercially available untagged PA-IL (PA-ILU) is typically purified by exploiting its natural affinity for Sepharose 4B [28,32], but alteration of the protein–carbohydrate binding specificity could prevent purification in this manner. One of the first steps required for this study was therefore the incorporation of an affinity tag that would enable simple and rapid purification of recombinant PA-IL (rPA-IL) proteins independently of glycan binding specificity. The *lecA* gene, encoding the wild-type PA-IL protein, was therefore cloned into two *E. coli* plasmid expression vectors to enable expression of rPA-IL with either an amino terminal (rPA-ILN) or carboxy terminal (rPA-ILC) polyhistidine (6HIS) tag and thereby enabling purification by IMAC. Both proteins were expressed to high levels in the soluble cytoplasmic fraction of *E. coli* KRX from which they were subsequently purified by IMAC. Assessment of the proteins by SDS-PAGE verified that both exhibited very high levels of purity (Fig. 2) and yields were typically around 800 mg/L of culture.

3.2. Structural and functional assessment of poly-histidine tagged rPA-IL proteins

The impact of the incorporated 6HIS tags on the quaternary structure and functionality of the rPA-IL proteins was assessed initially by gel permeation chromatography (GPC). We first determined experimentally the molecular weight of commercially obtained untagged PA-IL (PA-ILU) which is known to be a tetramer of four identical subunits under physiological conditions (Fig. 1) [28,33]. This was used as a reference for comparison with the rPA-IL proteins to determine their quaternary structure. The rPA-ILC protein was determined to be tetrameric, but the rPA-ILN protein was determined to exist as dimers indicating that the incorporation of the 6HIS affinity tag at the N-terminus of the protein had disrupted the quaternary structure of the protein (Supplementary Fig. S2). The functionality and carbohydrate binding properties of the rPA-IL proteins were assessed and compared to that of the PA-ILU protein using the hemagglutination assay. The rPA-ILC protein was found to have a comparable activity to PA-ILU in hemagglutination assays with both proteins fully agglutinating papain-treated rat red blood cells (RBCs) at a lectin concentration of 195 ng/mL (Supplementary Fig. 3A). Both proteins also showed comparable inhibition profiles for all sugars assessed in sugar inhibition assays (Supplementary Fig. S3B). The rPA-ILN protein was significantly less effective at agglutinating RBCs, requiring a concentration of 6.25 μg/mL to produce full agglutination. This was also more readily inhibited by all of the sugars evaluated in sugar inhibition assays. Hemagglutination assays confirmed that both of the rPA-IL proteins were functional, and differences in their comparative performance reflected the differences in their respective quaternary structures.

3.3. Selection of a target rPA-IL molecule for mutagenesis studies

The steric accessibility of the 6HIS tags within the quaternary structures of the rPA-IL proteins was assessed by ELLA. Both of the rPA-IL

proteins were tested for their ability to bind an immobilized Galα1–3Gal–BSA neoglycoprotein with subsequent detection of the bound lectins using an anti-HIS antibody [8]. Biotinylated GSLI, a plant lectin with a binding specificity for terminal α-galactose [10,34], was included in the assays as a positive control. Binding of both rPA-ILN and GSLI could be detected in ELLAs with high sensitivity, but binding of the rPA-ILC could not be detected using an anti-HIS antibody, even at relatively high lectin concentrations of 10 μg/mL (data not shown). As the functionality of both of the rPA-IL proteins had already been confirmed, this was therefore likely to be due to steric unavailability of the 6HIS tags within the rPA-ILC tetramer to binding by the anti-HIS antibody. This was further confirmed by direct immobilization of the rPA-ILC protein in ELISA plates and probing with anti-HIS antibody which failed to generate signals (data not shown). While incorporation of a 6HIS tag at the amino terminus of the rPA-IL was shown to disrupt the natural tetrameric structure of the PA-IL protein, the resulting dimeric molecules were demonstrated to be functional and could be readily detected, with high sensitivity, in ELLAs using an anti-HIS antibody. The pQE30PA-IL vector was therefore selected as the target DNA molecule for mutagenesis as the production of mutagenized rPA-IL proteins with amino terminally positioned 6HIS tags (rPA-ILNm) would not only facilitate simplified purification but also enable analysis of their carbohydrate binding activities through the use of ELLA assays without the need for any prior *in vitro* labelling steps. As all of the mutagenized proteins would ultimately be compared to the parental rPA-ILN protein and would therefore be expected to have equivalent quaternary structures, comparative analysis could be performed by ELLA to identify proteins with altered carbohydrate binding properties.

3.4. Mutagenesis of the rPA-ILN protein

Residues from three separate parts of the PA-IL monomer are involved in coordinating calcium and binding of the iGb3 trisaccharide Galα1–3Galβ1–3Glc [28] (Fig. 1). Amino acid residues Asp100, Thr104, Asn107, Asn108 of the calcium binding loop (residues 100–108), and Tyr36 of the neighbouring loop, are involved in coordination of the calcium ion and contribute interactions with the non-reducing α-linked galactose. Residues His50 and Gln53 do not participate in calcium coordination but contribute interactions with the non-reducing αGal and Gln53 also interacts with the penultimate galactose in the trisaccharide. Amino acid residues involved in the coordination of the essential calcium ion were not selected for mutagenesis since alteration of these residues would likely result in loss of calcium coordination and consequently result in loss of carbohydrate binding. As residues His50 and Gln53 are only involved in making contacts with the carbohydrate, these residues were selected as target amino acid residues for mutagenesis. The intervening Pro51 and Asp52 residues do not directly interact with bound carbohydrate, but modification of these residues could result in alterations in the overall conformation of the carbohydrate binding pocket and the spatial arrangement of the His50 and Gln53 residues. Proline residues introduce kinks and rigidity into polypeptide strands. Alteration of this residue might therefore be expected to result in dramatic structural changes in the carbohydrate binding site to negatively impact carbohydrate binding, and so this residue was not selected for substitution in this study. However, substitution of the Asp52 residue might have more subtle affects, and so this residue was selected for inclusion in the mutagenesis study.

The pQE30PA-IL plasmid was mutagenized using a PCR based method that resulted in the introduction of simultaneous random substitutions at positions corresponding to residues His50, Asp52 and Gln53 in the PA-IL protein. A total of 154 individual mutant clones were picked at random into 2 deep well 96 well plates to create matrices of clones expressing rPA-ILNm proteins. A number of different glycoproteins were used as immobilized targets in ELLA screens to identify clones expressing mutated rPA-ILNm proteins exhibiting altered binding specificities compared to the parental rPA-ILN protein. Glycoproteins used in this screen were selected to represent targets displaying key glycan epitopes: fetuin (3 complex N-linked and 3 O-linked glycan structures highly sialylated with terminal α2–3 and α2–6Neu5Ac) [35], asialofetuin (N and O-linked glycans with terminal β1–4 and β1–3 galactose repsectively), thyroglobulin (20 N-linked glycosylation sites) [36,37] and invertase (high mannose structures) [38]. PA-IL is known not to bind strongly to these glycoprotein targets [39], and so any rPA-ILNm proteins identified as generating altered responses to these targets were considered to have altered carbohydrate binding properties. Of the 154 clones screened, none of the rPA-ILNm proteins displayed significant binding to invertase or fetuin indicating that none of the mutants exhibited specificity for glycans with terminal mannose or sialic acid. However, a large number of rPA-ILNm proteins were observed to exhibit altered binding to asialofetuin and thyroglobulin. A total of 28 clones displayed significant binding to asialofetuin (generating ELLA signals above 0.4 au), and 9 additional clones showed significant binding to both asialofetuin and thyroglobulin (data not shown). A number of the rPA-ILNm proteins that exhibited strong binding to both asialofetuin and thyroglobulin, and some that exhibited selectivity for asialofetuin, were recovered and carried forward for further analysis. Selected rPA-ILNm proteins were named according to the well from which they were recovered in the original 96 well plates (i.e. rPA-ILNmE6 was recovered from row E, column 6).

3.5. Qualitative analysis of isolated rPA-ILNm proteins

Each of the rPA-ILNm proteins identified in the initial matrix screens was purified by IMAC to enable further characterization. The quaternary structure of each of the rPA-ILNm proteins was first assessed by GPC, and all of the proteins were observed to exist as dimers and therefore exhibited a comparable structure to the parental rPA-ILN protein (data not shown). As the proteins were purified by IMAC, and not on the basis of the proteins inherent functionality, purified protein preparations could have potentially contained a proportion of inactive protein. This could have a significant impact on the interpretation of data in subsequent characterization studies. To determine the percentage activity of each of the rPA-ILNm proteins, we exploited the observed binding of the rPA-ILNm proteins to asialofetuin in initial ELLA screens. A sample of each rPA-ILNm protein was injected onto a 1 mL asialofetuin sepharose column to determine the proportion of inactive (unbound protein) and active (bound) protein present in each preparation. For all of the rPA-ILNm preparations, no significant unbound protein peaks were observed, and >97% of the total protein injected was subsequently selectively eluted from the column by addition of 0.5 M galactose to the mobile phase (Supplementary Fig. 4). This selective elution confirmed that binding to the asialofetuin column was based on specific carbohydrate–protein interactions.

The specificity profile of the rPA-ILNm proteins was qualitatively assessed by performing ELLAs against a panel of 8 specific neoglycoproteins immobilized at a concentration of 5 μg/mL (Fig. 3). These enabled the detection of potentially weak interactions due to multivalent and high density display of glycan epitopes (average of 12 glycans per protein molecule)[7]. This screen clearly demonstrated that the RPLs identified exhibited a diverse range of carbohydrate binding specificities significantly altered compared to that of the parental rPA-ILN protein. The parental rPA-ILN protein displayed specificity for neoglycoproteins displaying Galα1–3Gal, Galα1–2Gal and GalNAc. In contrast, the rPA-ILNmC5, F6 and G3 RPLs exhibited specificity and selectivity for Galβ1–4GlcNAc–BSA (BSA–LacNAc) and did not display significant binding to the other neoglycoproteins tested. The rPA-ILNmE6 protein displayed strong binding to BSA–LacNAc and only weak binding to Galα1–3Gal–BSA and Galβ1–3GalNAc–HSA (HSA–T-antigen). Other RPLs displayed a capacity to bind a wider spectrum of neoglycoproteins. Of particular note was the rPA-ILNmB4

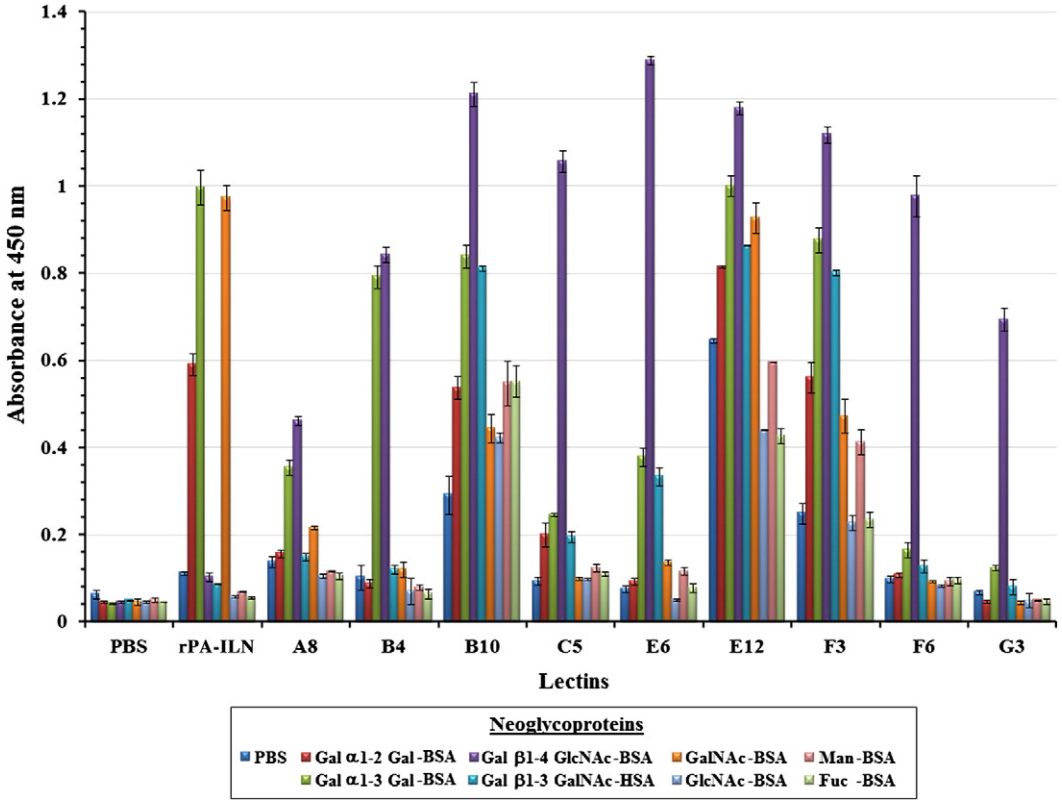

Fig. 3. Specificity analysis of rPA-ILNm proteins tested against specific neoglycoproteins. Qualitative ELLA analysis was performed against a range of specific neoglycoproteins immobilized at a concentration of 5 μg/mL. This demonstrated that the isolated rPA-ILNm proteins collectively exhibited a diverse range of binding specificities with respect to galactoslyated glycans.

protein which exhibited significant binding to Galα1–3Gal–BSA and BSA–LacNAc but, unlike the parental rPA-ILN protein, it did not exhibit binding to either the Galα1–2Gal–BSA or GalNAc–BSA. The rPA-ILNmB10 and rPA-ILNmF3 proteins displayed an even wider specificity profile. The strongest signals generated by these two proteins were in binding to BSA–LacNAc, but they also displayed strong binding to neoglycoproteins with terminal α-linked galactose and some binding towards GalNAc–BSA. Unlike the other rPA-ILNm proteins, the rPA-

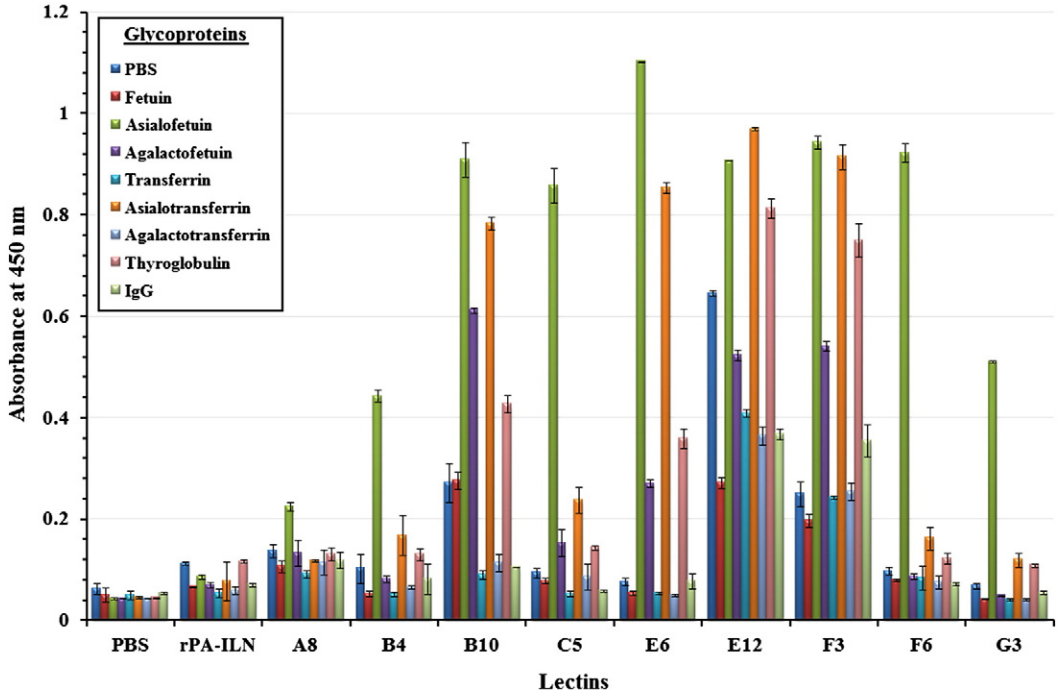

Fig. 4. Specificity analysis of rPA-ILNm proteins tested against specific glycoproteins. Qualitative ELLA analysis was performed against a range of natural glycoproteins and derived glycoforms immobilized at a concentration of 5 μg/mL. The observed binding of rPA-ILNm proteins to asialofetuin and asialotransferrin and the subsequent loss of binding to agalactofetuin and agalactotransferrin confirmed that binding was dependent on the terminal β1–4-linked galactose. Residual signals observed for rPA-ILNmB10 and rPA-ILNmF3 against agalactofetuin were potentially due to the presence of T-antigen [Galβ1–3GalNAc] which is also present on this glycoprotein.

Lectin	Sequence Alignment	Neoglycoprotein Specificity Profile
rPA-ILN	QGDRE – H P D Q – GLICH	Galα1-3Gal = GalNac > Galα1-2Gal
rPA-ILNmE12	QGDRE – G P C R – GLICH	----
rPA-ILNmF3	QGDRE – V P C R – GLICH	Galβ1-4GlcNAc (LacNAc) > Galα1-3Gal = Galβ1-3GalNAc (T-Antgen) > Gala1-2Gal = GalNAc = Man > Fuc = GlcNAc
rPA-ILNmB10	QGDRE – V P C E – GLICH	Galβ1-4GlcNAc (LacNAc) > Galα1-3Gal = Galβ1-3GalNAc (T-Antgen) > Galα1-2Gal = Man = Fuc > GalNac = GlcNAc
rPA-ILNmG3	QGDRE – V P N N – GLICH	Galβ1-4GlcNAc (LacNAc)
rPA-ILNmB4	QGDRE – T P N R – GLICH	Galβ1-4GlcNAc (LacNAc) > Galα1-3Gal
rPA-ILNmE6	QGDRE – N P N G – GLICH	Galβ1-4GlcNAc (LacNAc) > >> Galα1-3Gal = Galβ1-3GalNAc (T-Antgen)
rPA-ILNmC5	QGDRE – N P T S – GLICH	Galβ1-4GlcNAc (LacNAc)
rPA-ILNmA8	QGDRE – L P H R – GLICH	Galβ1-4GlcNAc (LacNAc) > Galα1-3Gal (Overall weak binding)
rPA-ILNmF6	QGDRE – P P R L – GLICH	Galβ1-4GlcNAc (LacNAc)

Fig. 5. Sequence alignment and neoglycoprotein specificity profile of rPA-ILNm proteins. A sequence alignment of amino acid residues from Gln45 to His59 of the parental rPA-ILN with the equivalent residues present in isolated rPA-ILNm proteins is shown. Specific amino acid substitutions were observed to occur with high frequency. Substitutions occurring more than once at each of the positions corresponding to His50, Asp52 and Gln53 in the rPA-ILNm proteins are indicated in boxes.

ILNmF3 and rPA-ILNmB10 proteins also exhibited binding to HSA–T-antigen. The rPA-ILNmE12 protein showed very high background signals in negative control wells with no immobilized neoglycoprotein which made it difficult to fully assess the data obtained. However, this protein appeared to display a specificity profile similar to that of the rPA-ILNmB10 and rPA-ILNmF3 proteins.

We further assessed the glycan specificity profile of the identified RPLs by performing qualitative screens against a broad range of natural glycoproteins and derived glycoforms immobilized at a concentration of 5 μg/mL (Fig. 4). These natural glycoproteins displayed glycans at lower densities than the neoglycoproteins. Data obtained using these targets therefore gave a greater, and more biologically relevant, insight into the binding activities and dependencies of the rPA-ILNm proteins.None of the rPA-ILNm proteins bound to fetuin or transferrin confirming that these RPLs could not bind to glycans with terminal sialylation. However, all of the rPA-ILNm proteins displayed strong binding to asialofetuin confirming their ability to bind to glycans displaying terminal β-linked galactose and LacNAc. Removal of terminal β1–4 linked galactose, by treatment with β1–4 galactosidase, eliminated the binding of the majority of the RPLs to the agalactofetuin glycoform. Only the rPA-ILNmB10 and rPA-ILNmF3 proteins displayed significant binding to the agalactofetuin glycoform. This was likely to be due to their ability to bind to O-linked T-antigen known to be present on the glycoprotein and confirmed their ability to bind to this glycan epitope in a true biological context.

Transferrin has only two N-linked biantennary complex glycans [35]. The rPA-ILNmE6, B10 and F3 proteins exhibited strong binding to the asialotransferrin glycoform which would display N-linked glycans with terminal LacNAc. As observed for the fetuin glycoforms, binding of these rPA-ILNm proteins was eliminated against the agalatotransferrin glycoform confirming that binding was dependent on the presence of the terminal β1–4 linked galactose. Interestingly, the rPA-ILNmB4, C5, F6 and G3 proteins, that had displayed strong binding to the asialofetuin glycoform, did not exhibit significant binding to the asialotransferrin glycoform. As all of the rPA-ILNm proteins were known to exhibit a comparable quaternary structure, and valency; this indicated that these RPLs displayed a lower overall relative affinity for terminal LacNAc and that effective binding was potentially more dependent on glycan density, or the protein context in which glycan epitopes were presented, and on avid binding. In addition to those shown in Fig. 4, the rPA-ILNm proteins were also tested against a number of other glycoproteins. This included RNase B [40], glucose oxidase [41] and invertase [38] that are known to display high mannose glycan structures and ovalbumin which is known to display hybrid structures [37]. None of the rPA-ILNm proteins displayed significant binding to these targets (data not shown).

3.6. Identification of amino acid substitutions in selected rPA-ILNm proteins

Plasmid DNA from each of the rPA-ILNm expressing clones was isolated and sequenced to determine the nature of the amino substitutions present in each protein (Fig. 5). It can be clearly seen that the selection of clones based on their strong binding to asialofetuin and thyroglobulin in the initial functional ELLA library screening process resulted in the identification of a collection of rPA-ILNm proteins in which specific amino acid substitutions occurred with high frequency at each of the mutagenized positions. Of the nine rPA-ILNm proteins isolated, three (rPA-ILNmB10, F3 and G3) were found to have an H50V substitution and two (rPA-ILNmE6 and C5) had an H50N substitution. Examining the Asp52 position, it can be seen that three rPA-ILNm proteins (rPA-ILNmB10, E12 and F3) were found to have a D52C substitution, while another three (rPA-ILNmB4, E6 and G3) had a D52N substitution. Also, arginine was found to be substituted for Gln53 in four rPA-ILNm proteins (rPA-ILNmA8, B4, E12 and F3). We undertook a more detailed analysis of this collection of rPA-ILNm proteins to ascertain the potential significance of these amino acid substitutions.

3.7. Lectin dose–response curves for defined neoglycoprotein targets

The carbohydrate binding properties of the selected rPA-ILNm proteins were further assessed by generating lectin dose–response curves against three specific neoglycoprotein targets; BSA–LacNAc, HSA–T-antigen and Galα1–3Gal–BSA (Fig. 6A, B, and C respectively). The BSA–LacNAc and Galα1–3Gal–BSA neoglycoproteins were immobilized at a concentration of 1 μg/mL, while the HSA-T-antigen was immobilized at a concentration of 5 μg/mL. As all of the lectin molecules to be assessed had an equivalent quaternary structure, these lectin dose–response curves enabled comparative analysis of the relative affinity of each of the rPA-ILNm lectins for each of the neoglycoproteins.

The parental rPA-ILN protein only showed very weak binding to BSA–LacNAc, even at relatively high lectin concentrations of 10 μg/mL. This was expected since the PA-IL protein is known not to bind significantly to glycans with terminal β1–4 linked galactose [28,39]. Conversely, all of the rPA-ILNm proteins, with the exception of the rPA-ILNmA8, displayed strong binding to BSA–LacNAc. Of particular

Fig. 6. Examination of the relative affinity of rPA-ILNm proteins for defined neoglycoproteins and glycoprotein targets. The relative affinities of rPA-ILNm proteins were comparatively assessed by performing lectin dilution plots against (A) BSA–LacNAc, 1 μg/mL; (B) HSA–T-antigen, 5 μg/mL; (C) Galα1–3Gal–BSA, 1 μg/mL; (D) asialofetuin, 5 μg/mL; (E) asialotransferrin, 5 μg/mL. The data obtained clearly demonstrated that the rPA-ILNmE6 protein exhibited high relative affinity and selectivity for glycans displaying terminal β1–4 linked galactose and LacNAc.

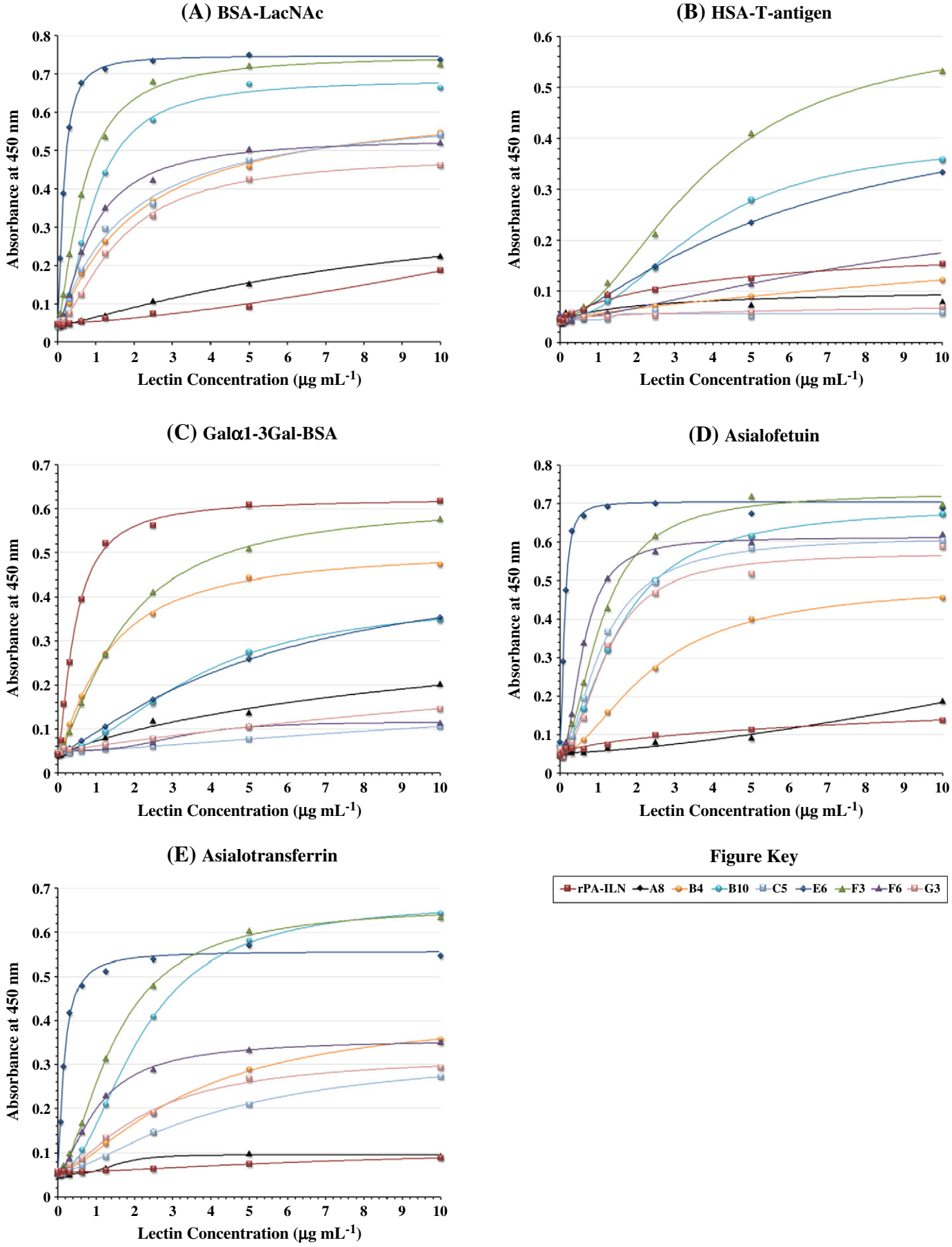
(A) BSA-LacNAc
(B) HSA-T-antigen
(C) Galα1-3Gal-BSA
(D) Asialofetuin
(E) Asialotransferrin
Absorbance at 450 nm
Lectin Concentration (μg mL-1)
Figure Key
rPA-ILN
A8
B4
B10
C5
E6
F3
F6
G3

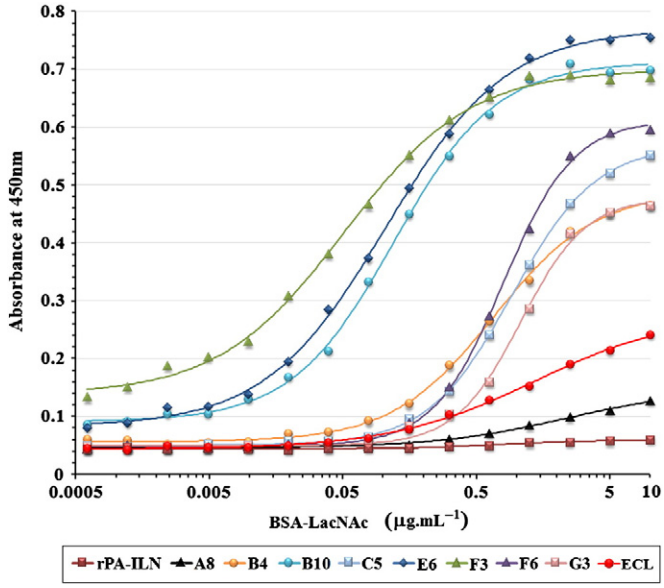

Fig. 7. Determination of affinity constants for rPA-ILNm proteins against BSA–LacNAc. Both rPA-ILNmF3 and rPA-ILNmE6 displayed higher relative affinities for BSA–LacNAc than ECL as indicated by their lower calculated K_D values. The rPA-ILNmF3 and rPA-ILNmE6 proteins generated K_D values of 0.42 nM and 1.15 nM respectively, while ECL generated a K_D value of 12.25 nM (Table 2). This indicates that the rPA-ILNmF3 and rPA-ILNmE6 proteins have approximately a 30 and 10 fold higher relative affinity for BSA–LacNAc, respectively, than ECL.

Table 2
Calculated B_{max} and K_D values for rPA-ILNm proteins.

Lectin	Conc. μg/mL	B_{max} (au)	½ B_{max} (au)	K_D μg/mL	K_D nM
rPA-ILNmA8	2	0.147	0.074	0.78	11.01
rPA-ILNmB4	2	0.490	0.245	0.54	7.57
rPA-ILNmB10	2	0.712	0.356	0.09	1.31
rPA-ILNmC5	2	0.570	0.285	0.80	11.30
rPA-ILNmE6	2	0.770	0.385	0.08	1.15
rPA-ILNmF3	2	0.700	0.350	0.02	0.42
rPA-ILNmF6	2	0.612	0.306	0.72	10.08
rPA-ILNmG3	2	0.478	0.239	0.94	13.26
rPA-ILN	2	0.060	0.030	ND	ND
ECL	4	0.280	0.140	0.87	12.25

note was the rPA-ILNmE6 protein which displayed a very high relative affinity to BSA–LacNAc, indicated by a very rapid increase in signal strength with increasing lectin concentration, and signals ultimately reached saturation at lectin concentrations above 1 μg/mL. The rPA-ILNmF3 and rPA-ILNmB10 proteins also showed a high relative affinity for BSA–LacNAc. The rPA-ILNmF3 protein displayed the highest relative affinity for HSA–T-antigen. The rPA-ILNmE6 protein displayed a significantly lower relative affinity for the HSA-T-antigen, and the remaining rPA-ILNm proteins did not display significant affinity for this neoglycoprotein.

The rPA-ILN protein displayed a significantly higher relative affinity to the Galα1–3Gal–BSA neoglycoproteins than any of the rPA-ILNm proteins. However, some of the rPA-ILNm proteins also displayed a capacity to bind strongly to this neoglycoproteins. Of these, the rPA-ILNmF3 and rPA-ILNm4 proteins displayed the highest relative affinity to the Galα1–3Gal–BSA neoglycoprotein. The rPA-ILNmE6 protein showed some capacity to bind the Galα1–3Gal–BSA neoglycoprotein but only at relatively high lectin concentrations and signal strengths did not reach saturation over the lectin concentration range examined. The rPA-ILNmB10 protein had displayed strong binding to the Galα1–3Gal–BSA neoglycoprotein in qualitative screens generating signals comparable to that of the rPA-ILNmF3 protein (Fig. 3). However, in lectin dose–response experiments, the rPA-ILNmB10 protein displayed a significantly lower relative affinity for this neoglycoprotein than rPA-ILNmF3, and it generated a response curve similar to that observed for the rPA-ILNmE6 protein. As the concentration of Galα1–3Gal–BSA neoglycoprotein used in lectin dose–response experiments was significantly lower than that used in the qualitative screens (1 μg/mL versus 5 μg/mL), this indicated that rPA-ILNmB10 actually exhibited a lower relative affinity for Galα1–3Gal–BSA than rPA-ILNmF3 and that effective binding was potentially more dependent on avid binding. The remaining rPA-ILNm proteins showed very little binding to Galα1–3Gal–BSA even at relatively high lectin concentrations of 10 μg/mL.

The data obtained from assays against the neoglycoproteins clearly showed that while some of the rPA-ILNm proteins, like rPA-ILNmE6, rPA-ILNmF6, rPA-ILNmC5 and rPA-ILNmG3, exhibited greater selectivity towards BSA–LacNAc, others, like rPA-ILNmF3 and rPA-ILNmB4, exhibited wider carbohydrate binding specificities for both α-linked and β-linked galactose.

3.8. Lectin dose–response curves for natural glycoprotein glycoforms

Lectin dose–response curves were also generated against asialofetuin and asialotransferrin immobilized at a concentration of 5 μg/mL (Fig. 6D & E respectively). The rPA-ILNmE6 protein displayed a high relative affinity for both asialofetuin and asialotransferrin with lectin dose–response curves reaching saturation for both glycoproteins at lectin concentrations above 1 μg/mL. Interestingly, while the remaining rPA-ILNm proteins were observed to bind strongly to asialofetuin, only the rPA-ILNmF3 and rPA-ILNmB10 proteins exhibited strong binding to asialotransferrin. The remaining rPA-ILNm proteins exhibited significantly lower binding to asialotransferrin even at relatively high lectin concentrations above 5 μg/mL. This indicated that binding of these proteins to glycans displaying terminal β1–4 linked galactose was potentially more dependent on the density or distribution of glycans, and possibly more reliant on avid binding, than rPA-ILNmE6.

3.9. Determination of affinity constants for rPA-ILNm proteins

A relative affinity constant, K_D, was calculated for selected rPA-ILNm proteins against the BSA–LacNAc neoglycoprotein essentially according to the method described by Kirkeby et al. (2002). K_D is defined as being the concentration of the neoglycoprotein required to

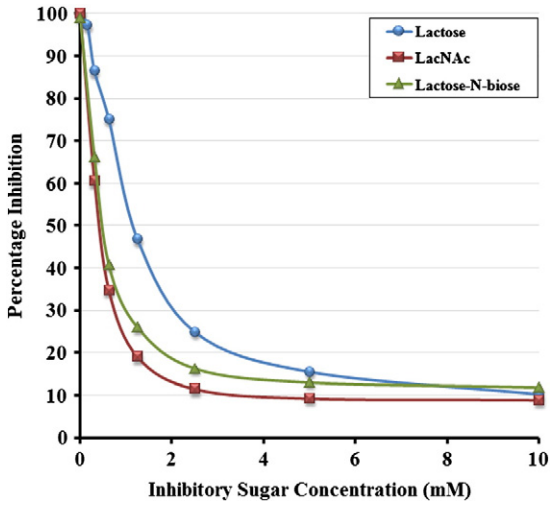

Fig. 8. Examining the linkage specificity of the rPA-ILNmE6 protein. Sugar inhibitions demonstrated that lactose, LacNAc and lactose-N-biose sugars were all capable of effectively inhibiting the binding of the rPA-ILNmE6 protein to a BSA–LacNAc neoglycoprotein target in ELLAs. This indicates that rPA-ILNmE6 can bind both terminal β1–4 and β1–3 linked galactose. The selectivity of rPA-ILNmE6 for BSA–LacNAc over HSA–T-antigen is therefore likely to be due to the terminal galactose being linked to a GlcNAc rather than GalNAc.

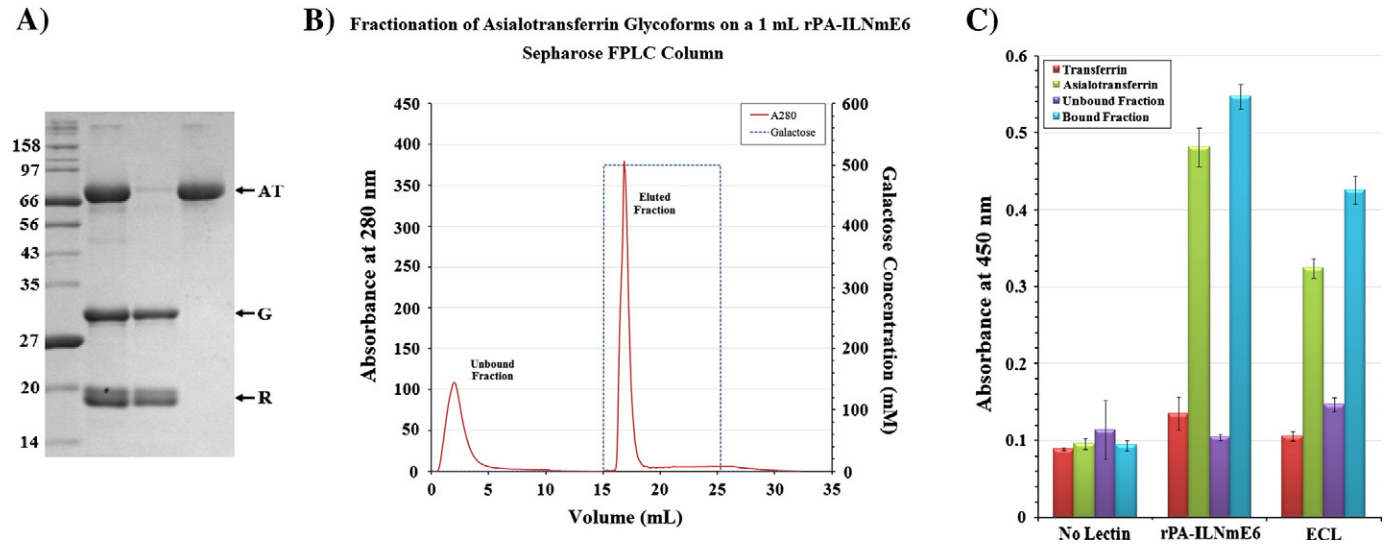

Fig. 9. The application of rPA-ILNmE6 for the separation and selective purification of glycoproteins and glycoforms displaying terminal β1–4 linked galactose. (A) SDS-PAGE analysis of fractions obtained from lectin pull down assays performed using rPA-ILNmE6 functionalized magnetic particles.: Lane 1—molecular weight ladder (NEB Wide Range Protein Ladder—sizes are in kDa); Lane 2—starting protein mix comprised of (AT) asialotransferrin [80 kDa], (G) non-glycosylated GFP [27 kDa] and (R) RNaseB [14 kDa]; Lane 3—unbound protein fraction; Lane 4—galactose eluted bound protein fraction. This clearly demonstrated the selective extraction of asialotransferrin from the starting protein mixture. (B) Separation of glycoprotein glycoforms: a 2 mL sample comprised of a mixture of 1 mg of transferrin and 1 mg of asialotransferrin was applied to a 1 mL rPA-ILNmE6 Sepharose FPLC column. The sample was effectively separated into two fractions: one fraction comprised of unbound protein (U) and one comprised of bound protein (Bd) which was selectively eluted by inclusion of 0.5 M galactose in the mobile phase. (C) ELLA analysis of FPLC fractionated transferrin glycoforms. Only the bound fraction elicited strong responses from the galactophilic lectins confirming effective separation and isolation of the asialotransferrin glycoforms.

fill half of the available lectin binding sites at equilibrium. If a lectin has a high relative affinity for the neoglycoprotein, then the K_D will be low as it will take a lower concentration of neoglycoprotein to bind half of the lectin molecules. A number of the rPA-ILNm proteins (rPA-ILNmE6, F3, B10 and B4) were shown to exhibit a significantly higher relative affinity for the BSA–LacNAc neoglycoprotein than that of the plant lectin ECL (Fig. 7 and Table 2)). Of particular note were the rPA-ILNmF3 and rPA-ILNmE6 proteins which generated K_D values of 0.42 nM and 1.15 nM respectively. This indicated that these proteins exhibited approximately a 30 and 10 fold higher relative affinity for the BSA–LacNAc neoglycoprotein, respectively, than ECL for which the calculated K_D was approximately 12.25 nM. The B_{max} values determined for the remaining rPA-ILNm proteins were significantly lower than those of rPA-ILNmF3 and rPA-ILNmE6 indicating that these proteins exhibited an overall lower relative affinity for the BSA–LacNAc neoglycoprotein. Fig. 7 also demonstrated that both the rPA-ILNmF3 and rPA-ILNmE6 proteins enabled a significantly greater sensitivity for detection of the BSA–LacNAc neoglycoprotein than ECL without the need for any prior labelling through biotinylation. Their ability to detect lower concentrations of immobilized BSA–LacNAc may also reflect a lower dependency for avid binding compared to the other rPA-ILNm proteins evaluated.

3.10. Examination of the linkage specificity of the rPA-ILNmE6 protein

Both the qualitative ELLA screens and the lectin dilution plots clearly demonstrated that the rPA-ILNmE6 protein exhibited selectivity for LacNAc and the protein did not exhibit significant binding to glycans displaying terminal α-linked galactose. The rPA-ILNmE6 protein also displayed a significantly higher relative affinity for BSA–LacNAc compared to HSA–T-antigen. The lower relative affinity for T-antigen could potentially be attributed to the β1–3 linkage of the terminal galactose; however, it could also have been due to the impact of the penultimate sugar residue i.e. GalNAc rather than a GlcNAc. To specifically examine the linkage specificity of the rPA-ILNmE6 protein in greater detail, we performed carbohydrate inhibition assays using lactose (Galβ1–4Glc), LacNAc (Galβ1–4GlcNAc) and lactose-N-biose (Galβ1–3GlcNAc) (Fig. 8). This demonstrated that binding of rPA-ILNmE6 to an immobilized BSA–LacNAc neoglycoprotein could be effectively inhibited by all three disaccharides. LacNAc and lactose-N-biose displayed similar inhibition profiles, and lactose was only slightly less effective. This indicated that the rPA-ILNmE6 had a capacity to bind to both terminal β1–4 and β1–3 linked galactose with a slight preference for linkage to GlcNAc rather than glucose. The lower relative affinity displayed by rPA-ILNmE6 for T-antigen structures was therefore more likely due to a reduced ability to accommodate the penultimate GalNAc moiety in the binding site.

3.11. Application of immobilized rPA-ILNmE6 for glycoprotein and glycoform isolation

To evaluate the ability of rPA-ILNmE6 to be used for selective glycoprotein and glycoform isolation and purification, the lectin was immobilized onto both magnetic particles and CNBr-activated Sepharose. The lectin was readily immobilized at high densities, and lectin immobilization densities of approximately 10 mg/mL and 20 mg/mL were achieved on the magnetic beads and the Sepharose resin, respectively. To evaluate the ability of the lectin functionalized magnetic particles to isolate glycoproteins displaying terminal β1–4 galactose, pull down assays were performed in 1.5 mL tubes using a test protein mixture prepared by mixing asialotransferrin with recombinant green fluorescent protein (GFP) (non-glycosylated protein) and RNase B. Fractions of unbound and bound protein were ultimately evaluated by SDS-PAGE (Fig. 9A). It could be clearly seen that the rPA-ILNmE6 magnetic beads selectively and efficiently extracted the asialotransferrin from the protein mixture and the protein was effectively recovered by the incorporation of free galactose into elution buffers. The rPA-ILNmE6 Sepharose resin was packed into 1 mL FPLC column housings to enable easy attachment to FPLC systems. The ability of this column to efficiently separate transferrin and asialotransferrin glycoforms was evaluated using a test sample containing a mixture of equal amounts of each glycoform. This test sample was injected onto the FPLC column and was separated

into two clear fractions, one unbound protein fraction and one galactose eluted protein fraction (Fig. 9B). Both the protein fractions were subsequently assessed by ELLA to evaluate their glycoform composition (Fig. 9C). Only the bound fraction was found to elicit responses from the galactophilic lectins, consistent with the ELLA responses of each of the initial individual starting test proteins, indicating that the rPA-ILNmE6 Sepharose column had efficiently separated the transferrin and asialotransferrin glycoforms into two distinct populations.

4. Discussion

The present study demonstrated for the first time how specific random mutagenesis strategies could be combined with a functional ELLA screening procedure to generate novel RPLs with diversified carbohydrate binding properties. The α-galactophilic PA-IL protein was exploited as a scaffold protein structure and the study demonstrated that its specificity could be significantly altered through the introduction of random substitutions at specific amino acid residues in the carbohydrate binding site. A panel of RPLs was generated that collectively exhibited a broad spectrum of different binding activities with respect to recognition of galactoslyated glycans. Some of these RPLs were found to exhibit broad carbohydrate binding specificities by binding to glycans with terminal β-linked and α-linked galactose, GalNAc and T-antigen (rPA-ILNmB4, rPA-ILNmF3 and rPA-ILNmB10) (Fig. 3). Others displayed greater selectivity towards glycans with terminal β1–4 linked galactose and LacNAc (rPA-ILNmC5, G3, F6 and E6). Isolated rPA-ILNm proteins, in particular rPA-ILNmF3 and rPA-ILNmE6, were shown to exhibit a significantly higher relative affinity for LacNAc than that of commercially available plant lectin ECL which is also specific for glycans with terminal β1–4 linked galactose (Fig. 7 and Table 2). These RPLs were also demonstrated to enable highly sensitive detection of the BSA–LacNAc neoglycoprotein, significantly greater than that possible with the plant lectin ECL, without the need for any prior labelling through biotinylation (Fig. 7). The ability of both LacNAc and lactose-N-biose to effectively inhibit binding of rPA-ILNmE6 protein to glycoprotein targets (Fig. 8) demonstrated that this RPL could bind to both terminal β1–4 and β1–3 linked galactose. The selectivity of rPA-ILNmE6 towards glycoproteins displaying glycans with LacNAc, and not T-antigen, was therefore more likely due to the terminal galactose of T-antigen structures being linked to a GalNAc moiety rather than GlcNAc.

4.1. The structural basis for altered carbohydrate binding properties of isolated rPA-ILNm proteins

In initial ELLA functional screens mutant clones expressing rPA-ILNm proteins with altered binding specificity for glycans with terminal β1–4 linked galactose and LacNAc were recovered at a very high frequency (37 clones out of 154 clones screened). Examination of the structures of the PA-IL protein reported to date [28,33] suggested that the His50 residue may sterically restrict oligosaccharides with terminal β-linked galactose from entering the binding pocket and therefore play a critical role in defining the α-galactophilic specificity of the wild-type PA-IL protein. Substitution of this His50 residue with a broad range of smaller, or less bulky, amino acids would possibly alleviate such steric hindrance and might explain the high frequency of occurrence of mutant clones expressing rPA-ILNm proteins capable of binding glycans displaying terminal β1–4 linked galactose in ELLA screens. However, specific His50 substitutions were recovered with high frequency in the isolated set of rPA-ILNm proteins. This implied that these substitutions not only alleviated potential steric hindrance imposed by His50 but also specifically promoted high binding to terminal β1–4 linked galactose and LacNAc. The high frequency of occurrence of these substitutions in the isolated rPA-ILNm proteins was likely biased due to the selection of clones based on binding to specific target glycoproteins displaying these glycan epitopes. However, this also demonstrated the utility of a functional screening approach for isolating novel RPLs exhibiting optimal carbohydrate binding properties for desired glycan targets.

4.2. The role of specific amino acid substitutions in dictating carbohydrate binding properties

Of the rPA-ILNm proteins identified, the rPA-ILNmE6 protein appeared to exhibit a high relative affinity for BSA–LacNAc. While this protein also showed some capacity to bind to the HSA–T-antigen and Galα1–3Gal–BSA neoglycoproteins, it only did so relatively weakly when compared to its response to the BSA–LacNAc (Fig. 6A, B and C) and only generated significant responses at relatively high RPL concentrations above 5 μg/mL. The rPA-ILNmC5 also appeared to bind well to BSA–LacNAc, albeit not as well as rPA-ILNmE6, but was not observed to bind significantly to the other neoglycoproteins. When these two proteins were examined against asialofetuin and asialotransferrin (Fig. 6D & E), it became clear that the rPA-ILNmE6 potentially had a significantly higher affinity for terminal β1–4 linked galactose and LacNAc than the rPA-ILNmC5 protein which appeared to be more dependent on the density of glycan display and potentially on avid binding. The rPA-ILNmC5 protein carries the same H50N substitution present in rPA-ILNmE6 but different substitutions at the Asp52 and Gln53 positions. These results indicate that while the H50N substitution may be associated with high affinity binding to terminal β1–4 linked galactose and LacNAc, the D52N and Q53G substitutions present in rPA-ILNmE6 play a role in further modulating its carbohydrate binding properties resulting in its significantly higher relative binding affinities for these glycan epitopes compared to rPA-ILNmC5.

The responses of another group of rPA-ILNm proteins indicated that an H50V substitution could also support high affinity binding to terminal β1–4 linked galactose and LacNAc. This substitution was present in rPA-ILNmF3, rPA-ILNmB10 and rPA-ILNmG3, and all of these proteins were observed to bind strongly to BSA–LacNAc. Analysis against asialofetuin and asialotransferrin again indicated however that the rPA-ILNmF3 and rPA-ILNmB10 proteins displayed a higher relative affinity for terminal β1–4 linked galactose and LacNAc than the rPA-ILNmG3. The rPA-ILNmF3 and rPA-ILNmB10 proteins also displayed strong binding to Galα1–3Gal–BSA, and were the only RPLs to display significant binding to the HSA–T-antigen neoglycoprotein, in qualitative ELLAs. This was not observed for the rPA-ILNmG3 protein. As these three proteins only differ from each other by possessing different substitutions at positions 52 and 53, this again demonstrates that amino acids at these positions play a role in further defining the specificity and affinity of the rPA-ILNm proteins. The rPA-ILNmF3 and rPA-ILNmB10 proteins only differed from each other at one position, carrying a Q53R and a Q53E substitution respectively. The Q53R substitution was also present in rPA-ILNmB4 which also bound well to the Galα1–3Gal–BSA neoglycoprotein. This data indicated that substitution of Gln53 with arginine or glutamic acid could be linked with the ability of these RPLs to bind α-linked galactose.

Another interesting observation was that while the lectin dose–response curves for rPA-ILNmF3 and rPA-ILNmB10 proteins on asialotransferrin did not increase as rapidly as that of rPA-ILNmE6, indicative of a lower relative affinity, they ultimately reached a higher absorbance plateau indicating a greater final density of these proteins bound to the surface. However, we had observed that both of these proteins had a tendency to form aggregates when high protein concentration stock solutions, stored at −80 °C, were being defrosted. These aggregates generally went back into solution when samples were fully thawed, but all samples were centrifuged to ensure removal of any residual protein aggregates prior to use. These proteins occasionally also generated high signals in negative control wells. This was also observed for the rPA-ILNmE12 protein, albeit more consistently, leading to it being excluded from further analysis. The one common feature of all three of these proteins was the occurrence of a D52C substitution, and

it is possible that this residue could mediate protein aggregation at high lectin concentrations through disulfide bond formation. As a result, the higher signals obtained for these lectins on asialotransferrin may be the result of binding of protein aggregates formed at high lectin concentrations or cross linking of target bound dimers at the plate surface effectively contributing to more avid binding.

Through the functional characterization of the RPLs isolated, and identification of the specific amino acid substitutions in each, we were able to identify specific substitutions at each of the mutagenized positions in the parental rPA-ILN protein that were linked with specific carbohydrate binding activities. However, this work also demonstrated that the ultimate specificity profile obtained for individual RPLs was dependent on the combined effect of substitutions at all three of the mutagenized positions within a given RPL carbohydrate binding site. This demonstrates the validity of implementing site-specific mutagenesis strategies with functional screening procedures to identify RPLs exhibiting desired and optimal carbohydrate binding properties.

4.3. Novel glycoanalytical tools for applications in the life sciences

Lectins have found widespread applications within the field of glycobiology and have been implemented in a diverse range of formats to characterize the glycosylation status and to detect changes in glycosylation of biomolecules. Changes in the glycosylation of proteins or cell surfaces can be concurrent with, and indicative of, a change in the physiological status of a cell or the development of a disease state and can therefore be used as a means of diagnosis [5,6,14]. LacNAc is an important glycan epitope commonly displayed on cell surfaces and as part of the antenna of complex N-linked glycan structures of glycoproteins. For example, serum IgG's, unlike many other serum glycoproteins, are not heavily sialylated, and the N-linked glycans present in the Fc region of the glycoproteins usually bear biantennary glycans terminating in LacNAc [42,43]. A reduction in terminal β1–4 galactosylation of these N-linked glycans has been diagnostically linked with a number of autoimmune disorders including rheumatoid arthritis, and increased galactosylation indicates remission of the disease [42,44–46]. The RPLs generated in this study were clearly demonstrated to be capable of sensitively detecting glycoproteins displaying terminal β1–4 galactose and of being capable of differentiating between different glycoprotein glycoforms (Fig. 4). Lectin affinity chromatography (LAC) is also widely used for the separation and isolation of glycoproteins. With more than 50% of proteins being glycosylated, LAC is a particularly powerful tool for glycoproteomic analysis. Proteomic samples are highly complex, and glycoproteins in biological materials are often only present in very small quantities. Efficient isolation and pre-concentration of these molecules are essential for their identification and characterization. LAC is often also used as an initial step to pre-concentrate oligosaccharides, glycopeptides, or to separate glycoforms, prior to MS-based glycoanalysis [7,17–19]. This study clearly demonstrated that the novel galactophilic RPLs reported could be immobilized at high densities onto solid support matrices, such as magnetic particles and sepharose resins, to generate highly effective bioaffinity matrices enabling efficient separation and selective purification of glycoproteins and glycoforms displaying LacNAc (Fig. 9). The RPLs reported could therefore find widespread applications in the fields of functional glycomics and glycoproteomics. They may also have applications in the analysis and selective purification of biopharmaceutical products as many of these products are glycosylated molecules and variations in glycosylation can have a very significant impact on their physiochemical properties, efficacy, and immunogenicity [42,47–49]. In addition to the many potential analytical scale applications, the ability to readily scale the production of our novel RPLs could also enable them to ultimately overcome the many barriers that have limited the application of eukaryotic lectins and enable them to be applied at a production scale, in a way analogous to Protein A.

Supplementary data to this article can be found online at http://dx.doi.org/10.1016/j.bbagen.2014.01.020.

Acknowledgments

This work was co-funded by Enterprise Ireland and the European Regional Development fund (ERDF) under the National Strategic Reference Framework (NSRF) (Enterprise Ireland grant no: CF/2011/1052—ProLegere Program: Glycoseparation Solutions for the Life Science Industries). Funding was also provided by the Science Foundation Ireland (grant number: 08/SRC/B1412—Irish Separation Science Cluster).

References

[1] M. Ambrosi, N.R. Cameron, B.G. Davis, Lectins: tools for the molecular understanding of the glycocode, Org. Biomol. Chem. 3 (2005) 1593–1608.
[2] H. Lis, N. Sharon, Lectins: carbohydrate-specific proteins that mediate cellular recognition, Chem. Rev. 98 (1998) 637–674.
[3] N. Sharon, H. Lis, History of lectins: from hemagglutinins to biological recognition molecules, Glycobiology 14 (2004) 53–62.
[4] N. Sharon, Lectins: carbohydrate-specific reagents and biological recognition molecules, J. Biol. Chem. 282 (2007) 2753–2764.
[5] D. Mislovičová, P. Gemeiner, A. Kozarova, T. Kožár, I. Lectinomics, Relevance of exogenous plant lectins in biomedical diagnostics, Biologia 64 (2009) 1–19.
[6] P. Gemeiner, D. Mislovicová, J. Tkác, J. Svitel, V. Pätoprstý, E. Hrabárová, G. Kogan, T. Kozár, Lectinomics: II. A highway to biomedical/clinical diagnostics, Biotechnol. Adv. 27 (2009) 1–15.
[7] A. Wu, E. Lisowska, M. Duk, Z. Yang, Lectins as tools in glycoconjugate research, Glycoconj. J. 26 (2008) 899–913.
[8] R. Thompson, A. Creavin, M. O'Connell, B. O'Connor, P. Clarke, Optimization of the enzyme-linked lectin assay for enhanced glycoprotein and glycoconjugate analysis, Anal. Biochem. 413 (2011) 114–122.
[9] H.J. Kim, S.J. Lee, H.-J. Kim, Antibody-based enzyme-linked lectin assay (ABELLA) for the sialylated recombinant human erythropoietin present in culture supernatant, J. Pharm. Biomed. Anal. 48 (2008) 716–721.
[10] S. Kirkeby, D. Moe, Lectin interactions with α-galactosylated xenoantigens, Xenotransplantation 9 (2002) 260–267.
[11] J. Zhao, T.H. Patwa, W. Qiu, K. Shedden, R. Hinderer, D.E. Misek, M.A. Anderson, D.M. Simeone, D.M. Lubman, Glycoprotein microarrays with multi-lectin detection: unique lectin binding patterns as a tool for classifying normal, chronic pancreatitis and pancreatic cancer sera, J. Proteome Res. 6 (2007) 1864–1874.
[12] S. Angeloni, J.L. Ridet, N. Kusy, H. Gao, F. Crevoisier, S. Guinchard, S. Kochhar, H. Sigrist, N. Sprenger, Glycoprofiling with micro-arrays of glycoconjugates and lectins, Glycobiology 15 (2005) 31–41.
[13] R. Rosenfeld, H. Bangio, G.J. Gerwig, R. Rosenberg, R. Aloni, Y. Cohen, Y. Amor, I. Plaschkes, J.P. Kamerling, R.B.-Y. Maya, A lectin array-based methodology for the analysis of protein glycosylation, J. Biochem. Biophys. Methods 70 (2007) 415–426.
[14] J. Katrlík, J. Švitel, P. Gemeiner, T. Kožár, J. Tkac, Glycan and lectin microarrays for glycomics and medicinal applications, Med. Res. Rev. 30 (2010) 394–418.
[15] T. Zheng, D. Peelen, L.M. Smith, Lectin arrays for profiling cell surface carbohydrate expression, J. Am. Chem. Soc. 127 (2005) 9982–9983.
[16] S. Chen, T. Zheng, M.R. Shortreed, C. Alexander, L.M. Smith, Analysis of cell surface carbohydrate expression patterns in normal and tumorigenic human breast cell lines using lectin arrays, Anal. Chem. 79 (2007) 5698–5702.
[17] R. Qiu, F.E. Regnier, Use of multidimensional lectin affinity chromatography in differential glycoproteomics, Anal. Chem. 77 (2005) 2802–2809.
[18] H. Geyer, R. Geyer, Strategies for analysis of glycoprotein glycosylation, Biochim. Biophys. Acta (BBA) Protein Proteomics 1764 (2006) 1853–1869.
[19] Z. Yang, W.S. Hancock, Monitoring glycosylation pattern changes of glycoproteins using multi-lectin affinity chromatography, J. Chromatogr. A 1070 (2005) 57–64.
[20] C. Oliveira, J.A. Teixeira, L. Domingues, Recombinant lectins: an array of tailor-made glycan-interaction biosynthetic tools, Crit. Rev. Biotechnol. (2012) 1–15.
[21] P.R. Stancombe, F.C.G. Alexander, R. Ling, M.A. Matheson, C.C. Shone, J.A. Chaddock, Isolation of the gene and large-scale expression and purification of recombinant *Erythrina cristagalli* lectin, Protein Expr. Purif. 30 (2003) 283–292.
[22] D. Hu, H. Tateno, A. Kuno, R. Yabe, J. Hirabayashi, Directed evolution of lectins with sugar-binding specificity for 6-sulfo-galactose, J. Biol. Chem. 287 (2012) 20313–20320.
[23] R. Yabe, R. Suzuki, A. Kuno, Z. Fujimoto, Y. Jigami, J. Hirabayashi, Tailoring a novel sialic acid-binding lectin from a ricin-B chain-like galactose-binding protein by natural evolution-mimicry, J. Biochem. 141 (2007) 389–399.
[24] P.R. Romano, A. Mackay, M. Vong, J. deSa, A. Lamontagne, M.A. Comunale, J. Hafner, T. Block, R. Lec, A. Mehta, Development of recombinant *Aleuria aurantia* lectins with altered binding specificities to fucosylated glycans, Biochem. Biophys. Res. Commun. 414 (2011) 84–89.
[25] D.C. Propheter, L.K. Mahal, Orientation of GST-tagged lectins via in situ surface modification to create an expanded lectin microarray for glycomic analysis, Mol. Biosyst. 7 (2011) 2114–2117.

[26] N. Gilboa-Garber, V. Ginsburg, *Pseudomonas aeruginosa* lectins, Methods in Enzymology, vol. 83, Academic Press, 1982, pp. 378–385.
[27] A. Imberty, M. Wimmerova, E.P. Mitchell, N. Gilboa-Garber, Structures of the lectins from *Pseudomonas aeruginosa*: insights into the molecular basis for host glycan recognition, Microbes Infect. 6 (2004) 221–228.
[28] B. Blanchard, A. Nurisso, E. Hollville, C. Tétaud, J. Wiels, M. Pokorná, M. Wimmerová, A. Varrot, A. Imberty, Structural basis of the preferential binding for globo-series glycosphingolipids displayed by *Pseudomonas aeruginosa* Lectin I, J. Mol. Biol. 383 (2008) 837–853.
[29] A. Wu, J. Wu, M.-S. Tsai, Z. Yang, N. Sharon, A. Herp, Differential affinities of *Erythrina cristagalli* lectin (ECL) toward monosaccharides and polyvalent mammalian structural units, Glycoconj. J. 24 (2007) 591–604.
[30] L. Litterer, T. Schagat, Protein expression in less time: a short induction protocol for KRX, Promega Notes 96 (2007) 20–21.
[31] N. Gilboa-Garber, D. Sudakevitz, The hemagglutinating activities of *Pseudomonas aeruginosa* lectins PA-IL and PA-IIL exhibit opposite temperature profiles due to different receptor types, FEMS Immunol. Med. Microbiol. 25 (1999) 365–369.
[32] N. Gilboa-Garber, L. Mizrahi, N. Garber, Purification of the galactose-binding hemagglutinin of *Pseudomonas aeruginosa* by affinity column chromatography using sepharose, FEBS Lett. 28 (1972) 93–95.
[33] G. Cioci, E.P. Mitchell, C. Gautier, M. Wimmerova, D. Sudakevitz, S. Perez, N. Gilboa-Garber, A. Imberty, Structural basis of calcium and galactose recognition by the lectin PA-IL of *Pseudomonas aeruginosa*, FEBS Lett. 555 (2003) 297–301.
[34] A.M. Wu, S.C. Song, J.H. Wu, E.A. Kabat, Affinity of *Bandeiraea (Griffonia) simplicifolia* Lectin-I, Isolectin-B4 (BSI-B4) for Gala1-4Gal Ligand, Biochem. Biophys. Res. Commun. 216 (1995) 814–820.
[35] T. Iskratsch, A. Braun, K. Paschinger, I.B.H. Wilson, Specificity analysis of lectins and antibodies using remodeled glycoproteins, Anal. Biochem. 386 (2009) 133–146.
[36] J. Charlwood, H. Birrell, A. Organ, P. Camilleri, A chromatographic and mass spectrometric strategy for the analysis of oligosaccharides: determination of the glycan structures in porcine thyroglobulin, Rapid Commun. Mass Spectrom. 13 (1999) 716–723.
[37] H.-J. Jeong, Y.-G. Kim, Y.-H. Yang, B.-G. Kim, High-throughput quantitative analysis of total N-glycans by matrix-assisted laser desorption/ionization time-of-flight mass spectrometry, Anal. Chem. 84 (2012) 3453.
[38] R.B. Trimble, P.H. Atkinson, Structural heterogeneity in the $Man_{8-13}GlcNAc$ oligosaccharides from log-phase Saccharomyces yeast: a one- and two-dimensional ^1H NMR spectroscopic study, Glycobiology 2 (1992) 57–75.
[39] C.P. Chen, S.C. Song, N. Gilboa-Garber, K.S. Chang, A.M. Wu, Studies on the binding site of the galactose-specific agglutinin PA-IL from *Pseudomonas aeruginosa*, Glycobiology 8 (1998) 7–16.
[40] R.A. Dwek, Glycobiology: toward understanding the function of sugars, Chem. Rev. 96 (1996) 683–720.
[41] K. Takegawa, A. Konjo, H. Iwamoto, K. Fujiwara, Y. Hosokawa, I. Kato, K. Hiromi, S. Iwahara, Novel oligomannose-type sugar chains derived from glucose oxidase of *Aspergillus niger*, Biochem. Int. 25 (1991) 181.
[42] R. Jefferis, Glycosylation as a strategy to improve antibody-based therapeutics, Nat. Rev. Drug Discov. 8 (2009) 226–234.
[43] A. Beck, E. Wagner-Rousset, M.-C. Bussat, M. Lokteff, Klinguer-Hamour, Trends in glycosylation, glycoanalysis and glycoengineering of therapeutic antibodies and Fc-fusion proteins, Curr. Pharm. Biotechnol. 9 (2008) 482–501.
[44] D.R. Burton, R.A. Dwek, Sugar determines antibody activity, Science 313 (2006) 627–628.
[45] T.S. Raju, Terminal sugars of Fc glycans influence antibody effector functions of IgGs, Curr. Opin. Immunol. 20 (2008) 471–478.
[46] J.D. Marth, P.K. Grewal, Mammalian glycosylation in immunity, Nat. Rev. Immunol. 8 (2008) 874–887.
[47] G. Walsh, R. Jefferis, Post-translational modifications in the context of therapeutic proteins, Nat. Biotechnol. 24 (2006) 1241–1252.
[48] A.M. Sinclair, S. Elliott, Glycoengineering: the effect of glycosylation on the properties of therapeutic proteins, J. Pharm. Sci. 94 (2005) 1626–1635.
[49] R.G. Werner, K. Kopp, M. Schlueter, Glycosylation of therapeutic proteins in different production systems, Acta Paediatr. 96 (2007) 17–22.
[50] K. Arnold, L. Bordoli, J. Kopp, T. Schwede, The SWISS-MODEL workspace: a web-based environment for protein structure homology modelling, Bioinformatics 22 (2006) 195–201.
[51] S. McNicholas, E. Potterton, K.S. Wilson, M.E.M. Noble, Presenting your structures: the CCP4mg molecular-graphics software, Acta Crystallogr. D 67 (2011) 386–394.